Kinetic Stability and Spectroscope investigation of Octadecanoic Acid- 17-Oxo-Methyl Ester (OA17OME)

C.Prabhu[1],P.Rajesh[2]*, D.Vijayalakshmi[3],M. Parthasarathy[4] ,E.Dhanalakshmi[5],V. Gowthami[6]
[1,2,3,4,5,6] Department of Physics, School of Basic Sciences Vels Institute of Science Technology And Advance Studies Pallavaram, Chennai-600 117, Tamilnadu,India.
*** Corresponding author: rajesh.ncc5coy@gmail.com(P.Rajesh)**
Tel:+91 8189823556

ABSTRACT

The OA17OME have been synthesised from a methanol extract of Aeglemarmelos leaves. The theoretical and FT-IR spectrum values are highly correlated. The electrical, inter-molecular interaction and NBO characteristics of the title chemical were determined using Density Functional Theory (DFT) at the B3LYP/6-311G++ (d,p) level. UV-Vis spectroscopy measurements, as well as examination of energy levels and global softness were utilised to elucidate information about charge transport inside the molecule. The global reactivity descriptors and Frontier Molecular Orbitals (FMOs) have been computed and interpreted. The electron acceptor and donor regions are represent in the MEP and Mulliken population analysis on atomic charge is also computed and confirmed in Molecular Docking investigations.

Keywords: FMOs, B3LYP/6-311G ++ (d,p) ,OA17OME
DOI Number: 10.48047/NQ.2022.20.16.NQ88209 NeuroQuantology2022;20(16):2098-2112

1. Introduction

The molecular weight of OA17OME (312.48) and its Molecular Formula (C19H36O3). This plant is a member of the Rutaceae family and may be found in parts of South Asia and Southeast Asia. Because of their numerous therapeutic characteristics, ayurvedic medicinal plants are widely employed in Indian medicine. Several writers investigated the named substance and its derivatives. Hydroxylated molecules are of medicinal relevance in various illnesses characterised of by cell damage. Hydroxyoctadecadienoic acids are 10100 times more abundant in LDL (Low Density Lipoproteins) than in healthy people[1]. Adsorption of octadecanoic acid (CH3(CH2)16COOH) at C-face (0001) and R-face (11h02) sapphire is used to investigate the influence of head group/substrate interaction on SAM development. The unit cell area and Al3+ coordination of these two regularly used orientations differ greatly[2]. Stearic acid, methyl ester, or stearate is a saturated 19 carbon-chained molecule that is also known as octadecanoic acid methyl ester (OA). Fatty acids have diverse antiviral actions against viruses[3].The mass spectra of the pyrrole-oxides of the 16 isomeric oxooctadecanoic acids and the 17 hydroxyoctadecanoic acids and their TMS ethers have now been reported. Methyl 3-0x0-octadecanoate (2)t (600 mg, 1.9 mmol) was dissolved in a combination of ethanol (15 ml) and M-KOH (7 ml) and the solution was agitated overnight at room temperature. The ethanol was then extracted under decreased pressure, and the residue was mixed with

water (30 ml) and fed to a briskly fermenting baker's yeast suspension[4]. A review of the OA17OME literature There is no entire theoretical and experimental value of GC-MS,FT-IR, UV-Vis a spectroscopic research, as well as electro negativity,chemical potential,Electronic density were carried out by using Density Functional Theory (DFT) calculations based on DFT/B3LYP with 6-311G ++(d,p) basis set and addition molecular docking.

2 Materials and Methods

2.1 Plant Collection

The Aeglemarmelas leaves were collected from Thiruvallur District,Tamil Nadu, India.

2.2 Extractions

The Leaves of Aeglemarmelas were thoroughly washed in double distilled water and shed-dried powdered of (1.0 kg)was extracted with methanol at the room temperature. The solvent was completely removed by the rotary vacuum evaporator from the crude to extract the 40g of compound.

2.3 Experimental Details

2.3.1GC-MS

GC-MS analysis revealed that several compounds are present.I choose the OA17OME as shown in **Fig 1**in the range of m/z represents mass divided by charge number and the horizontal axis in a mass spectrum the peak value are 58.0000,98.0000,111.0000,etc.

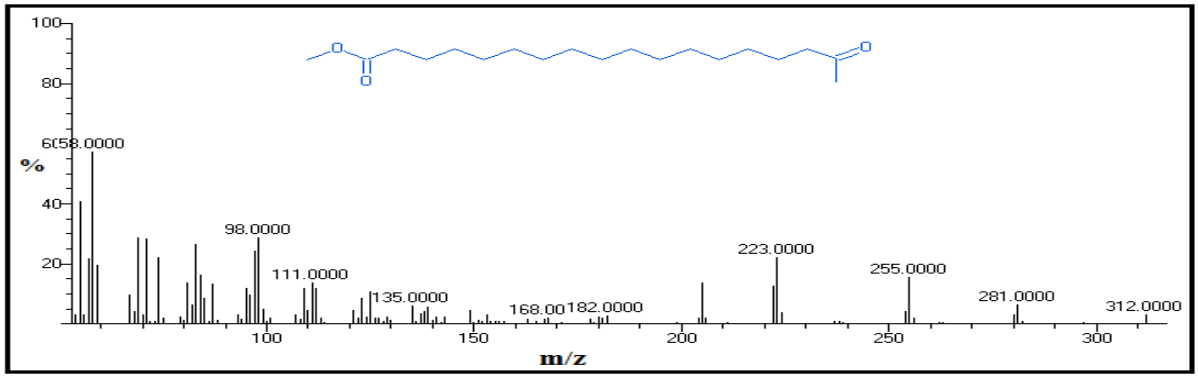

Fig1 GC-MS Chromatogram of methanol extract of Leaves of Aeglemarmelas (OA17OME)

2.3.2 FT-IR

The spectroscopic pure sample of OA17OMEwas produced from Aldrich chemicals, USA.And interpretations of experimental and theoretical data of Fourier Transform Infrared (FT-IR) spectra have the principle that when infrared (IR) radiation passes through a sample, some of the radiation is absorbed. The radiation through the sample is recordedin the region 4000–400 cm^{-1}.

2.3.2 UV–Vis

The UV-Vis absorption spectrometer is a valuable tool for researchers in chemistry, physics, material science, and biology.The UV-Vis spectrum is due to the electronic transitions of the molecule. This is characteristic of a compound. Qualitative and quantitative estimations of compounds are possible by this non destructive technique in IIT MADRAS.The spectrum was recorded in spectrophotometer in the range 200–400 nm.

3. Computations Approaches

In the present work, the Density Functional Theory (DFT/B3LYP) at the 6-311++G(d,p) basis set level was adopted to calculate the optimized parameters and vibrationwave numbers of the normal modes of the title molecule[5,6].The quantum chemical calculations were performed by applying DFT method usingGaussian 09W package and Beeke-3-Lee-Yang-Parr (B3LYP) supplemented with the standard 6-311++G(d,p) basis set.OtherMEP,Molecular Docking, Mulliken,electronic properties such as ionization potential, electron affinity,HOMO- LUMO band gap, electro negativity, hardness and softness were replicated at B3LYP/6-311++ G(d,p) level of theory [7].

4. Result and Discussion

4.1 Optimised structural parameters

Ground state optimized geometry of OA17OMEobtained by DFT/B3LYP with 6-311G ++ (d,p) basis set is shown in **Fig2**, along with the numbering of atoms and symbol.

OA17OME, we observe carbon bond between the $C_1$and O_{19}atom of bond length 1.21 A˚, this value is not mentioned in the experimental reported data. However, there is an intra-molecular hydrogen bonding available. InOA17OMEmolecule, we can predict (1.52 A˚)between $C_2$and C_3 as well as weak bonding between C_{22} and H $_{56}$ [1.08 A ˚].

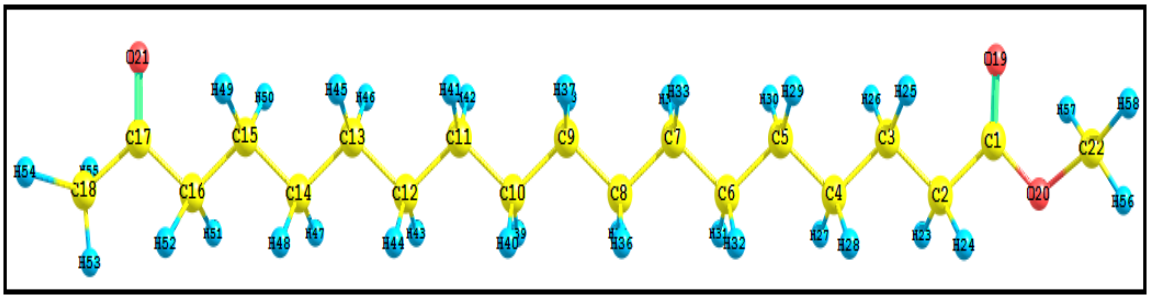

Fig2Optimized Structure of OA17OME

The main bond length values in the molecules show that there is a hydrogen bonding and the strength of the hydrogen bond is lower than theOA17OME compound. No proton transfer occurred during geometry optimization. The titled compound was found to have thirty five C-H bonds, thirteen C-C bonds, three C-O bonds and one O-C bonds. All the C,H and Obond lengths in the molecules are within the range of standard value (1.53 A˚). The calculated shortest value of bond length comes out of 1.080 A˚, which is quite less than the standard value (1.51 A˚) of C and O bond length. The C and H bond lengths remain between 1.51 A˚ to 1.52 A˚.

Table1 Optimized Geometrical Parameters of OA17OME

Bond length (Å)	B3LYP \6-311++G(d,p)	Bond length (Å)	B3LYP\6-311++G(d,p)
$C_1 - C_2$	1.51	$C_{10} - H_{40}$	1.09
$C_1 - O_{19}$	1.21	$C_{11} - C_{12}$	1.53
$C_1 - O_{20}$	1.35	$C_{11} - H_{41}$	1.09
$C_2 - C_3$	1.52	$C_{11} - H_{42}$	1.09
$C_2 - H_{23}$	1.09	$C_{12} - C_{13}$	1.53
$C_2 - H_{24}$	1.09	$C_{12} - H_{43}$	1.09
$C_3 - C_4$	1.53	$C_{12} - H_{44}$	1.09
$C_3 - H_{25}$	1.09	$C_{13} - C_{14}$	1.53
$C_3 - H_{23}$	1.09	$C_{13} - H_{45}$	1.09
$C_4 - C_5$	1.53	$C_{13} - H_{46}$	1.09
$C_4 - H_{27}$	1.09	$C_{14} - H_{15}$	1.53
$C_4 - H_{28}$	1.09	$C_{14} - H_{47}$	1.09
$C_5 - C_6$	1.53	$C_{14} - H_{48}$	1.09
$C_5 - H_{29}$	1.09	$C_{15} - H_{50}$	1.09
$C_5 - H_{30}$	1.09	$C_{16} - C_{17}$	1.52
$C_6 - C_7$	1.53	$C_{16} - H_{51}$	1.10
$C_6 - H_{31}$	1.09	$C_{16} - H_{52}$	1.10
$C_6 - H_{32}$	1.09	$C_{17} - C_{18}$	1.52
$C_7 - H_{33}$	1.09	$C_{17} - O_{21}$	1.21
$C_7 - H_{34}$	1.09	$C_{18} - H_{53}$	1.09
$C_8 - H_{36}$	1.09	$C_{18} - H_{54}$	1.09
$C_8 - H_{36}$	1.09	$C_{18} - H_{55}$	1.09

$C_9 - C_{10}$	1.53	$O_{20} - C_{22}$	1.43
$C_9 - H_{37}$	1.09	$C_{22} - H_{56}$	1.08
$C_9 - H_{38}$	1.09	$C_{22} - H_{57}$	1.09
$C_{10} - C_{11}$	1.53	$C_{22} - H_{58}$	1.09

4.2Vibrational Spectra

Vibrational spectral assignments have been performed on the recorded FT-IR (**Fig 3**)spectra based on theoretically predictablewave numbers by B3LYPmethod using 6-311++G(d,p) basis. The calculated vibrational wave numbers, measured FT-IR band positions and their tentative assignments are presented in **Table 2.**

4.2.1C-H Vibrations

The C-H stretching occurs above 3000 - 3100 cm^{-1} and is typically exhibited as a multiplicity of weak to moderate bands, compared with the C-H stretch[8]. In the present investigation theυCH stretching vibration has been found at 3100 cm^{-1}in FT-IR spectrawhich is further supported by the PED contribution of 99% and the values of these mode forOA17OME is 3097 cm^{-1}.The CCCH out of plane deformation is observed between 1000 and 700 cm^{-1}. The DFT calculation gives the mode at 967, and 738 cm^{-1}. The (CCH) in-plane deformation vibration is given at 1165, 1149cm^{-1} at B3LYP/6-311++G(d,p) method.

4.2.2 C=C,C-CVibrations

Generally, the C=C stretching vibrations are observed in the region of 1430–1650 cm^{-1}[9-11].The C=C stretching vibrations of titled compound are observed with very strong intensity of 1464cm^{-1}.The C-C vibration are most found in the range 1600-1400cm^{-1}[12].

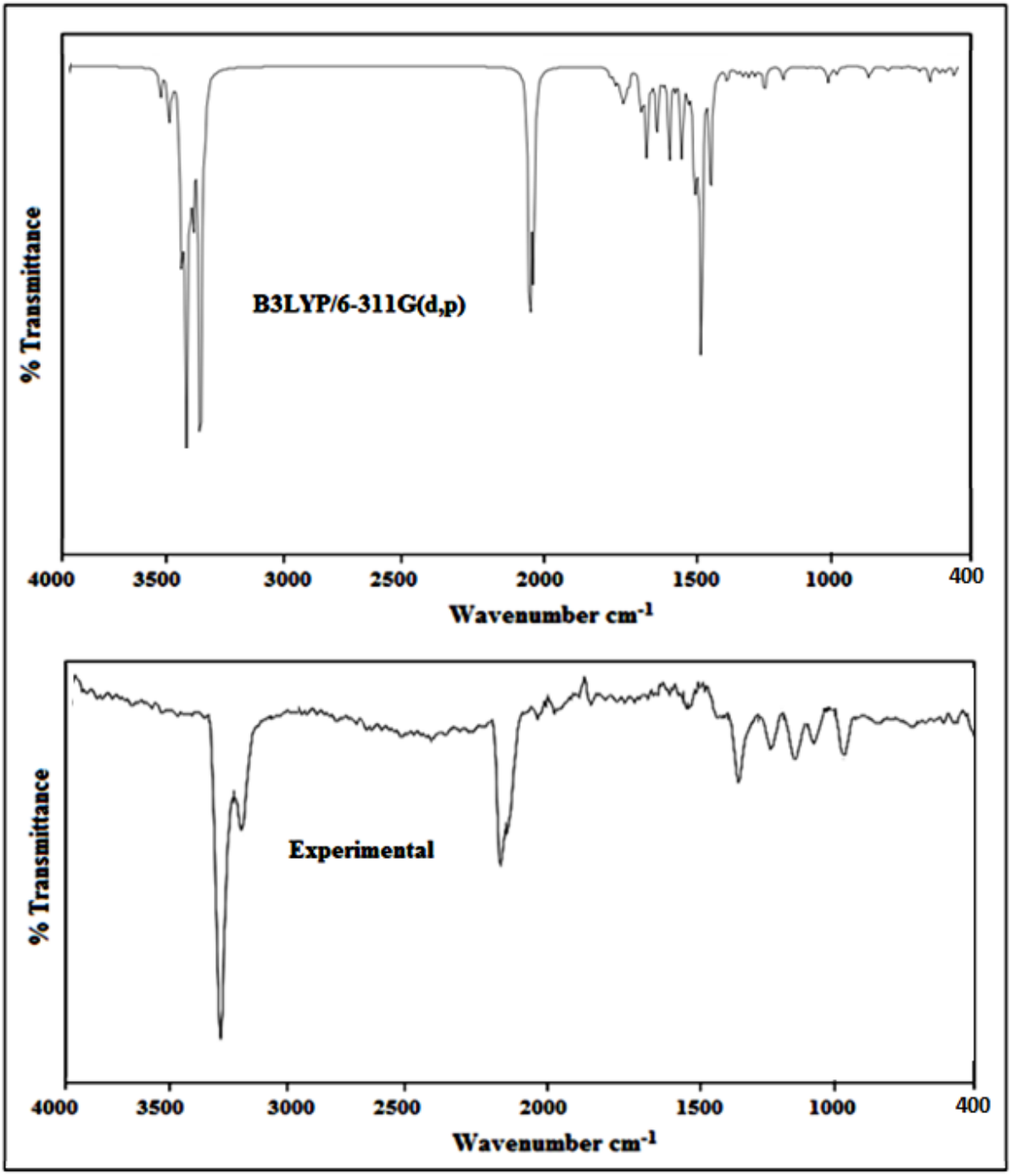

Fig 3 Vibrational Assignment of OA17OME

Table 2 Vibrational Assignment of OA17OME

Calculated B3LYP/6-311++G(d,p)	Experimental	Vibrational Assignments+(PED)
3172	3176	υCH_3(79)
3144	-	υCH(70)
3139	-	υCH_3(50)
3128	-	υCH(50)
3097	3100	υCH(99)
3093	-	υCH(43)
3073	-	υCH(11)
3070	-	υCH(26)

3063	-	υCH(100)
3055	-	υCH(100)
3053	-	υCH(82)
3051	-	υCH(96)
3050	-	υCH(10)
3041	-	υCH(84)
3037	-	υCH(12)
3035	3035	υCH(44)
3034	-	υCH(10)
3033	-	υCH(10)
3032	-	υCH(46)
3020	3016	υCH(48)
3011	-	υCH(22)
3009	-	υCH(42)
3008	-	υCH(26)
3006	-	υCH(50)
1811	-	υOC(91)
1726	1743	υOC(88)
1519	1525	δHCH(36)
1511	1512	δHCH(70)+ τHCOC(10)
1508	-	δHCH(26)
1498	-	δHCH(81)
1496	1493	δHCH(36)
1482	-	δHCH(76)
1475	-	δHCH(87)
1464	1472	δHCH(64) +τHCCC(12)+υCC(21)
1422	-	τHCCC(21)
1394	1393	δHCH(70)+υCC(16)
1336	-	δHCC(12)
1328	-	δHCC(21)
1319	-	δHCC(12)
1302	-	δHCC(10)
1214	1220	δHCH(13)+ τHCOC(21)
1199	1194	δOCO(11)
1179	-	δHCH(13)+τHCOC(40)
1165	-	υCC(14) +τHCC(11)
1149	1142	δHCC(33) + τHCCC(12)
1139	-	τHCCO(33)
1079	-	υCC(39)
1073	-	υCC(15)
1072	1067	υCC(29)
1069	-	υCC(21)
1068	-	υCC(24)
1065	1063	υCC(35)
1048	-	υCC(27)
1047	1037	υOC(87)
1025	-	υCC(24)
1018	-	υCC(10)
1004	-	υCCHC(90)
989	995	υCC(19)

984	-	υCC (27)
967	-	τHCCC(10)
901	-	υOC(26) + CC(25)
830	819	υCC(61)
738	740	τHCCC(28)+δCCC(17)
705	713	δOCO(33)+υOC(12)
590	-	υCC(27) + δOCC(40)
580	574	δHCC(72) + OUT OCOC(58)
526	-	δOCC(10)+ δCCC(14)
516	516	τCCC(16)
485	-	δCCC(12)
481	480	δHCC(12)
468	-	δOCC(11)+ δCCC(23)
403	-	δOCC(10)

The stretching vibrational bands for C-C bond are observed at 1450, 1440, 1430, 1420, 1410 and 1370 cm^{-1}. The CCC in-plane bending vibrations areobserved at 740 cm^{-1} and the out-of-plane bending vibrations are appeared at 574,516, 480 cm^{-1} [13,14].

4.2.3 C=O vibrations

Carbonyl stretching vibrations are expected to appear as medium or strong bands at 1715-1680 cm^{-1} [15]. In the present study, the band at 1743 cm^{-1} in FT-IR spectrum is attributed to the C=O stretching vibration of OA17OME, which is consistent with the calculated frequency at 1726 cm^{-1}.The out-of-plane bending mode of the C=O bond observed at 713cm^{-1} in FT-IR spectrum is very close to the computed value of 705 cm^{-1}, which is also confirmed by the PED values.

4.3 Natural-Bonding-Orbital (NBO) Analysis

The Natural bond orbital (NBO) program also makes extensive provision for energetic analysis of NBO interactions. The second order perturbation theory analysis of Fock matrix was carried out to evaluate the donoracceptor interactions in the NBO basis [16]. NBO analysis was conducted on this molecule at the DFT/B3LYP/ 6-311G++(d,p) level in order to elucidate the intramolecular, rehybridisation and delocalisation of electron density within the molecule which are presented in **Table 3**. Delocalisation of electron density between occupied Lewis-type (bond or lone pair) NBO orbitals and formally unoccupied (antibond or Rydgberg) non-Lewis NBO orbitals correspond to a stabilising donoracceptor interaction. This calculation is done by examining all possible interactions between 'filled' (donor) Lewis-type NBOs and 'empty'(acceptor) non-Lewis NBOs. The analysis ofOA17OME are showin **Table 3**.The intramolecularhyperconjugative interaction of σ(C_1-C_2) distributes to σ*(O_{20}-C_{22}), stabilization energy of 3.52 kJ/mol. The intramolecularhyperconjugative interactions of σ (C_2-H_{24}) orbital to σ* (C_1-O_{19}), σ(C_{18}-H_{54}) distributes σ*(C_{17}- C_{21}) leads to strong stabilization energy of 5.19 kJ/mol and 4.65 kJ/mol, respectively. The n → π* stabilization energies of lone pair of electrons present in the oxygen atom LP(O_{19}) to the anti bonding π*(C_1-O_{20}) show stabilization energy of 16.5 kJ/mol and 34.58 kJ/mol, respectively. The same LP(O_{20}), of the NBO conjugated with σ*(C_1-O_{19}) leads to an enormous stabilization of 49.34 kJ/mol as shown in **Table 3**. This is the highest energy from all interactions.

Table 3 NBO analysis of OA17OME

Donor NBO (i)	Acceptor NBO (j)	E(2) Kcal / mol	E(j) - E(i) a.u.	F(i,j) a.u.
σC_1 -C_2	$\sigma^* O_{20}$ -C_{22}	3.52	0.86	0.049
σC_2 -C_3	$\sigma^* C_1$ -O_{20}	3.13	0.9	0.048
σC_2 –H_{23}	$\sigma^* C_1$ –O_{19}	5.19	0.48	0.047
σC_2 –H_{24}	$\sigma^* C_1$ –O_{19}	5.19	0.48	0.047

$\sigma C_{15} - H_{49}$	$\sigma^* C_{16} - H_{51}$	3.07	0.9	0.047
$\sigma C_{15} - H_{50}$	$\sigma^* C_{17} - O_{52}$	3.07	0.9	0.047
$\sigma C_{16} - H_{51}$	$\sigma^* C_{17} - O_{21}$	5.18	0.5	0.046
$\sigma C_{16} - H_{52}$	$\sigma^* C_{17} - O_{21}$	5.17	0.5	0.046
$\sigma C_{18} - H_{53}$	$\sigma^* C_{17} - O_{21}$	4.25	1.04	0.059
$\sigma C_{18} - H_{54}$	$\sigma^* C_{17} - O_{21}$	4.65	0.51	0.044
$\sigma C_{18} - H_{55}$	$\sigma^* C_{17} - O_{21}$	4.64	0.51	0.044
LPO_{19}	$\sigma^* C_1 - C_2$	16.5	0.65	0.095
LPO_{19}	$\sigma^* C_1 - O_{20}$	34.58	0.56	0.126
LPO_{20}	$\sigma^* C_1 - O_{19}$	7.29	1.09	0.08
LPO_{20}	$\sigma^* C_1 - O_{19}$	49.34	0.3	0.109
LPO_{20}	$\sigma^* C_{22} - H_{57}$	3.9	0.75	0.051
LPO_{20}	$\sigma^* C_{22} - H_{58}$	3.9	0.75	0.051
LPO_{21}	$\sigma^* C_{16} - C_{17}$	18.48	0.65	0.099
LPO_{21}	$\sigma^* C_{17} - C_{18}$	18.79	0.63	0.098

4.4 Molecular Electrostatic Potential

The electronic density is connected to the molecular electrostatic potential (MEP), which is a particularly valuable descriptor in understanding locations for electrophilic attack and nucleophilic reactions, as well as hydrogen bonding interactions [17]. The MEP surface was produced using the B3LYP/6-311++G(d,p) approach to anticipate reactive sites for the title compound's electrophilic and nucleophilic processes. The electrostatic potentials at the surface were shown in Fig 4.The colour code of these maps is in the range between –0.0759a.u (deepest red) to + 0.0363a.u (deepest blue) in OA17OME. Red colours parts represent the regions of negative electrostatic potential which is related to nucleophilic reactivity, while blue ones represent regions of positive electrostatic potential which is related to nucleophilic reactivity. From **Fig 4**, the negative potential value is -0.0198 a.u. for oxygen atom of carbonyl group. Maximum positive regions localized on the H atom of hydroxyl group have the value of +0.00827a.u. The H atoms have lower values than the hydroxyl group. As a result, the greatest attraction is shown by the H atoms. The greatest repulsion is shown by O atoms..

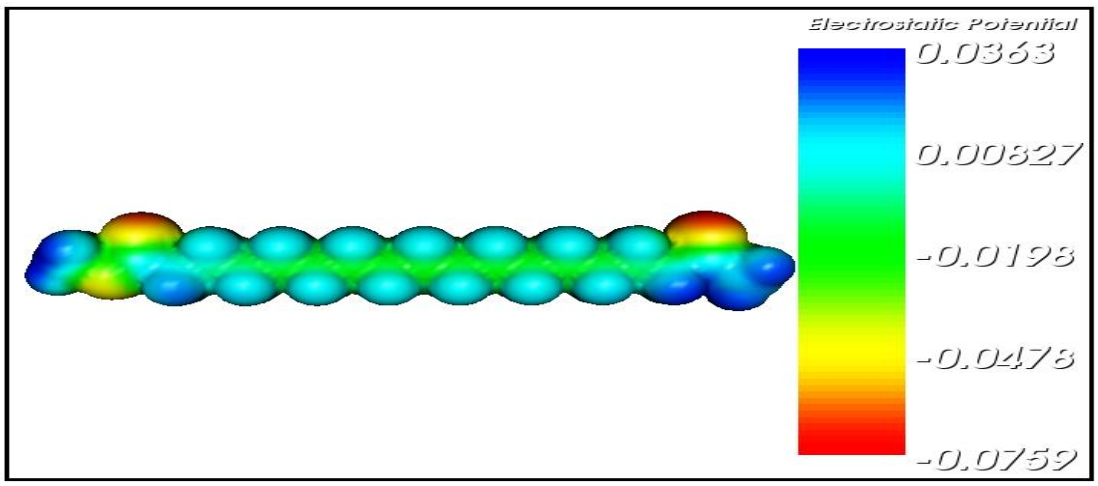

Fig4 Molecular Electrostatic Potential of OA17OME

4.5 MullikenPopulation Analysis

Mulliken atomic charge calculation is significant in the application of quantum chemical calculations to molecular systems because atomic charges affect dipole moment, molecule polarizability, electronic structure, and many other molecular systems. The charge distributions across the atoms point to the creation of donor and acceptor pairs involving the charge transmitting molecule. Table 4 shows the Mulliken population analysis of the OA17OME

molecule, which was derived using the B3LYP/6-311++G(d,p) basis set.

Table 4 Mulliken Charge ofOA17OME

Atoms	Charges (eV)	Atoms	Charges (eV)
C_1	0.6071	H_{30}	0.0973
C_2	-0.2682	H_{31}	0.0937
C_3	-0.1668	H_{32}	0.0806
C_4	-0.1796	H_{33}	0.0818
C_5	-0.1756	H_{34}	0.0949
C_6	-0.1746	H_{35}	0.0935
C_7	-0.1744	H_{36}	0.0804
C_8	-0.1743	H_{37}	0.0814
C_9	-0.1743	H_{38}	0.0944
C_{10}	-0.1742	H_{39}	0.0934
C_{11}	-0.1744	H_{40}	0.0803
C_{12}	-0.1745	H_{41}	0.0818
C_{13}	-0.1749	H_{42}	0.0949
C_{14}	-0.1790	H_{43}	0.0932
C_{15}	-0.1649	H_{44}	0.0801
C_{16}	-0.2683	H_{45}	0.0841
C_{17}	0.4185	H_{46}	0.0972
C_{18}	-0.3856	H_{47}	0.0922
O_{19}	-0.4793	H_{48}	0.0789
O_{20}	-0.4672	H_{49}	0.1014
O_{21}	-0.4427	H_{50}	0.1147
C_{22}	-0.0826	H_{51}	0.1235
H_{23}	0.1365	H_{52}	0.1099
H_{24}	0.1230	H_{53}	0.1072
H_{25}	0.1022	H_{54}	0.1357
H_{26}	0.1154	H_{55}	0.1504
H_{27}	0.0941	H_{56}	0.1187
H_{28}	0.0809	H_{57}	0.1357
H_{29}	0.0842	H_{58}	0.1215

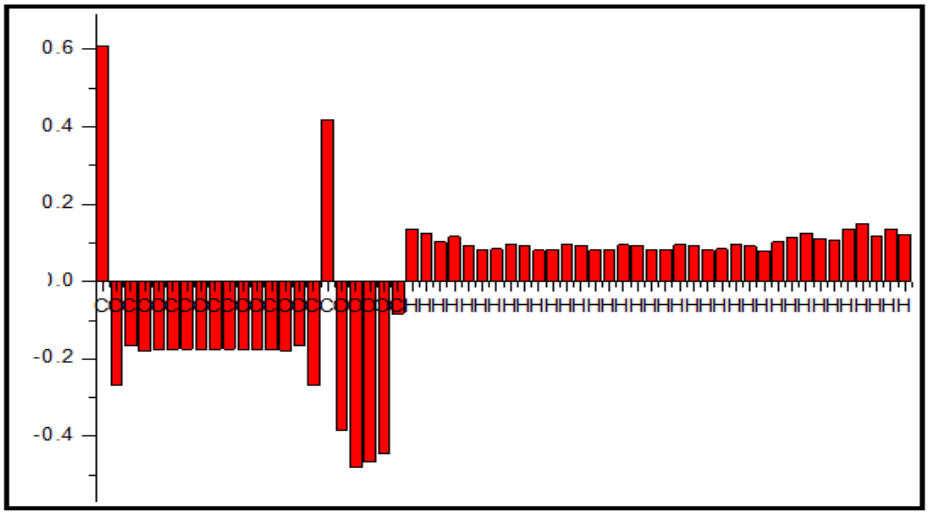

Fig 5 Atomic Charges of the OA17OME

The Mulliken charge analysis of OA17OME shows that the presence of oxygen atom (O_{19}= -0.479 , carbon atom (C_1 = 0.607) imposes positive charges on C_2, C_3, C_4, C_5,C_6, C_7, C_8, C_9, C_{10},C_{11}, C_{12}, C_{13}, C_{14}, C_{15}, C_{16} atoms. However, H_{23} ,H_{24}, H_{25}, H_{26}, H_{27}, H_{28}, H_{29}, H_{30}, H_{31}, H_{32}, H_{33}, to and H_{58} possess positive charge distributions due to large negative charges on carbon atoms C_2= -0.26827, C_3=-0.16682, C_4= -0.17964, C_5=-0.17567, C_6=-0.17462, C_7= -0.17445, C_8=-0.17435, C_9=-0.17439, C_{10}=-0.17428, C_{11}=-0.1744, C_{12}=-0.17451,C_{13}=-0.17493, C_{14}=-0.17902, C_{15}=-0.16492, C_{16}=-0.26833.The Mulliken atomic charge distributions are plottedin **Fig 5**.

4.6 UV-Visible

Ultraviolet spectra analyses have been calculated by B3LYP/6-311++G(d,p) method along with measuredUV–Visible dataand gas phase by theoretical calculation (Fig.6) have been used to determine the low-lying excited states of OA17OME. The **Table 5** which is mean for UV–Vis absorption shows three different possible transitions, with absorption maximum at 283.03, 217.13 and 190.28 nm respectively at gas phase. This observation is made clear in the theoretical UV–Vis spectrum which shows one peak at 280 nm with large absorption coefficient and one small peakat 220nm as shown in **Fig 6**.[18, 19]

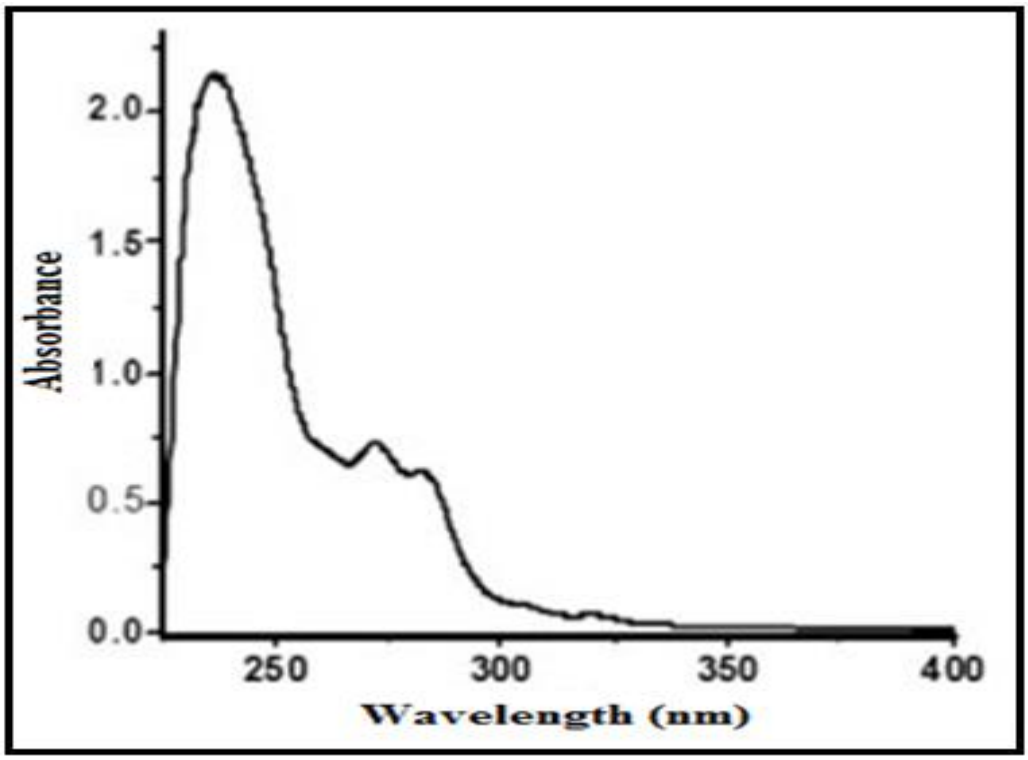

Fig6 UV-Visof OA17OME

Table 5.The UV-Vis excitation energy of OA17OME

States	**TD B3LYP/6-311++G(d,p)**		
	Gas phase		
	Exp	**λ_{cal}**	**E(ev)**
S_1	280	283.03	4.3805
S_2	220	217.13	5.7102
S_3	-	190.28	6.5160

5. Mathematical Determination of Energy Values

The highest occupied molecular orbital (HOMO) and Lowest unoccupied molecular orbital (LUMO) of the title compound are computed with same B3LYP/6-311G ++ (d,p) method and are shown in **Fig7.** The energy levels of HOMO and LUMO, energy gap are presented in **Table 6**. The electrophilicity index is a measure of decrease in total energy while electron sharing. In the title compound it is observed 1.843eV, which indicates the electron sharing in the molecule.

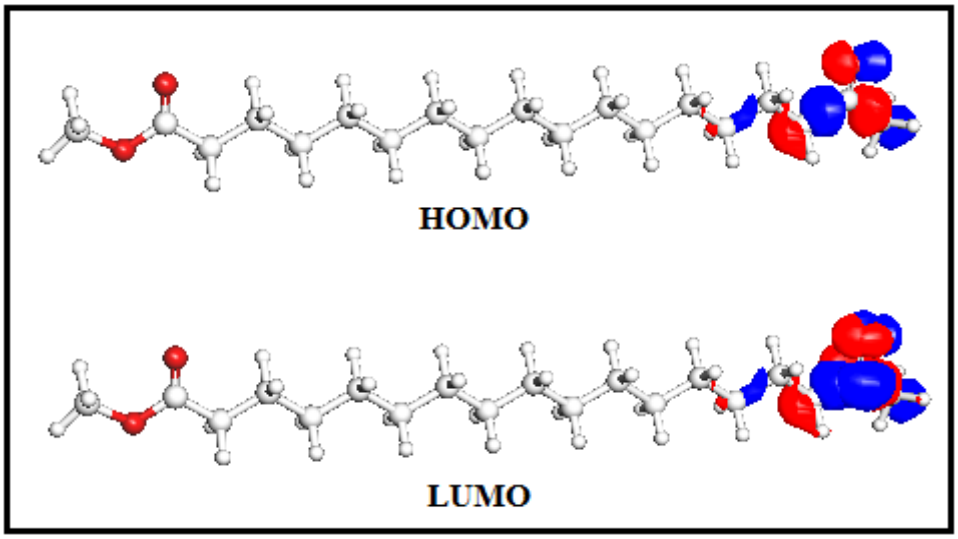

Fig7 HOMO-LUMO energy of OA17OME calculated at B3LYP/6-311++G (d, p)

The electro negativity of the title compound is3.4105eV, HOMO and LUMO diagrams show the charge distribution around the different types of donors and acceptors bonds presented in the molecule in the ground and first excited states respectively. The frontier orbital energy gaps (E_{LUMO} - E_{HOMO}) OA17OMEis found to be 6.3090eV in the gas phase. The HOMO energy level is 6.5650eV where as that of LUMO is 0.2560eV which indicate the molecule requires only a minimum energy to change the state from HOMO to LUMO. The global softness of the molecule is 0.3170eV whereas that of the hardness is 3.1545eV, which indicate the molecule is relatively hard so it tends to undergo changes or reactions easily. Gauss View 5.0.8 visualization program [20] has been utilized to construct the shapes of frontier molecular orbitals in **Table 6.**

Table 6 Calculated energy values of OA17OMEby B3LYP/6-311++G(d,p) method

Molecular Properties	Formula	B3LYP/6311++G(d,p)
Ionization potential (I)	I = - (HOMO)	+6.5650
Electron affinity (A)	A = - (LUMO)	-0.2560
Energy gap	Eg= HOMO - LUMO	6.3090
Electronegativity(χ)	$\chi = \frac{I+A}{2}$	3.4105
Chemical potential(μ)	$\mu = \frac{-(I+A)}{2}$	-3.4105
Chemical hardness(η)	$\eta = \frac{I-A}{2}$	3.1545
Chemical softness (S)	$S = \frac{1}{\eta}$	0.3170
Electrophilicity index (ω)	$\omega = \mu^2/2\eta$	1.8436

6.Molecular Docking

Molecular docking can held to great importance in the field of structural molecular biology, pharmacogenomics design and the most energetically favourable binding force of the interaction between the ligand and target protein as well as predicts the binding conformation and affinities of any species to target protein. AutoDock is an automated procedure for predicting the interaction of ligands with bio macromolecular targets. Molecular docking studies have been done using Maestro-10.2 docking program inbuilt in Schrödinger suite based on the Lamarckian genetic algorithm [21] was used to perform molecular docking investigations. The X-ray crystal structure of human VEGFR2 with a resolution of 1.93 Å was selected from the Research Collaboratory for Structural Bioinformatics protein data bank.The docking studies were carried out for using Maestro 10.2 docking program and the visualization of docking site. The grid box size of 100 × 100 × 100 points was set with a spacing of 0.79 Å

over the target protein binding pocket.The specific drug treatments against cancer are yet to be discovered. A greater negative value (-7.421 kcal/mol) of binding energy of any species reveals that it has the better docking ability to target protein as well as the docking of ligand and target protein were selected band on the related binding energy value.The predicted of C-H…O hydrogen bonding value NBO analysis, stabilises the protein ligand interaction. The amino acid residue ARG -1051, PRO -1057, ASP -1056, GLY -841, ASN -923, PHE -918, LEU – 899, and GLS -885 in the active site of the VEGFR2 protein interacts with the OA17OME molecule by C-H…O hydrogen bonding and stabilises the VEGFR2 ligand complex (**Fig8**,**9**). While, the presence of phenyl group in the OA17OMEmolecule increases its binding affinity. Out of 100 genetic algorithm runs, the best docked conformation had a binding energy of -7.421kcal/mol.

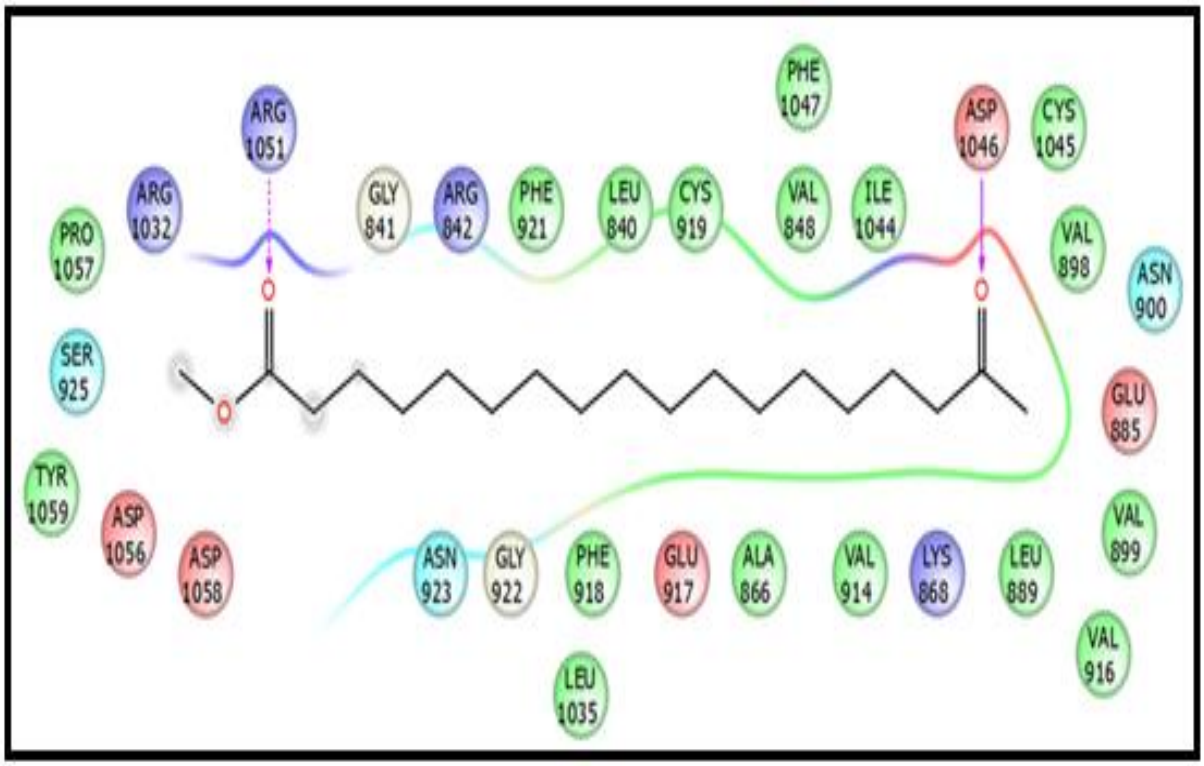

Fig8 Automated molecular docking of OA17OME angiotensin converting enzyme (ACE)

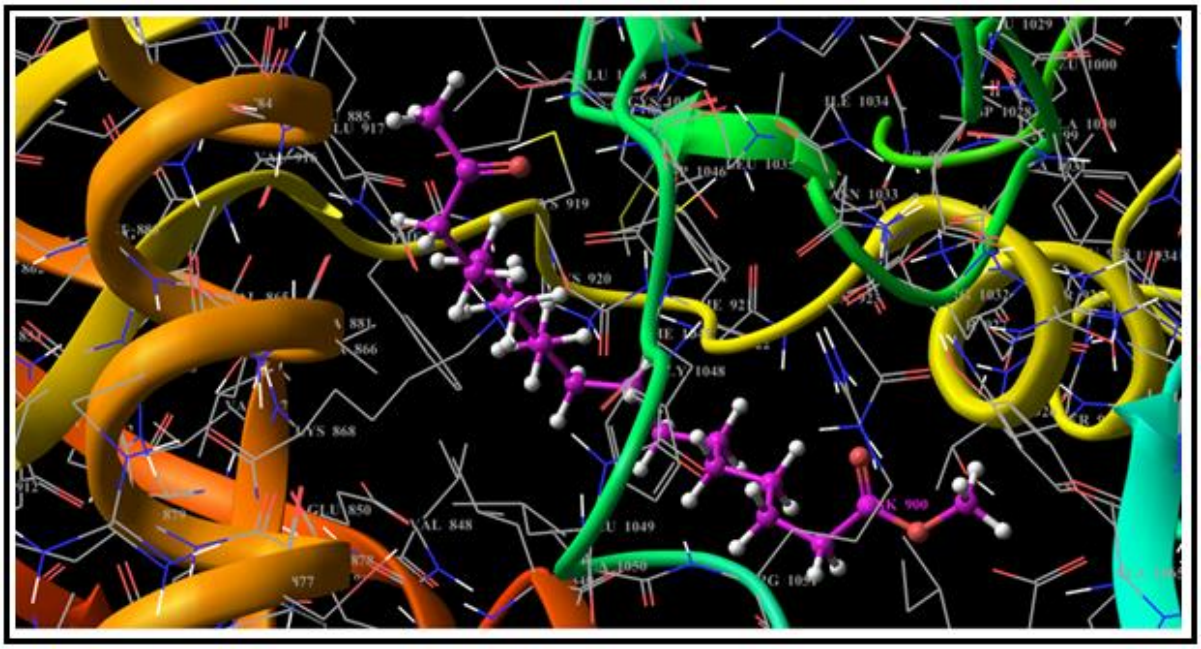

Fig9Molecular docking simulation of OA17OME with the selected protein

7. Conclusions

The optimized structural parameter such as bond lengths and bond angles are calculated. The experimental vibrational spectra are in good agreement with the theoretical spectra. The wave numbers obtained by TED calculations are in fair agreement with the observed values. The NBO analysis reveals the occurrence of hyperconjugative interaction and charge delocalization around the bonds. Theoretical electronic absorption spectra in gas space were compared with the experimental data and the molecular orbital coefficient analysis suggests π-π* type that electronic transitions. The HOMO-LUMO energy gap has a substantial influence on the ICT and the calculated value is 3.554eV. The lowering of HOMO- LUMO energy gap, a quantum chemical descriptor, explains the ease with which charge transfer interactions take place within the molecule. The MEP maps show that oxygen and nitrogen atoms are the negative potential sites and the positive potential sites are around the hydrogen atom.The molecular docking study concludes with the fact that the OA17OMEmolecular has might inhibitor activity against protein, which indicates against the human albumin receptor (HSA) as evident from the binding energy of-7.42 Kcal/mol. This result identifies the inhibitory activity against human albumin receptor.

References

1. Axelson M , O Larsson , 27-Hydroxylated Low Density Lipoprotein (Ldl) Cholesterol Can Be Converted To 7alpha,27-Dihydroxy-4-Cholesten-3-One (Cytosterone) Before Suppressing Cholesterol Production In Normal Human Fibroblasts. Evidence That An Altered Metabolism Of Ldl Cholesterol Can Underlie A Defective Feedback Control In Malignant Cells, J.Biol Chem. 271(22)(1996) 12724-12736.

2. Chad E. Taylor And Daniel K. Schwartzb ,Octadecanoic Acid Self-Assembled Monolayer Growth At Sapphire Surfaces , American Chemical Society.19 (7) (2003) 2665–2672.

3. Reagan Entigu Ak Linton , Jerah, Samuel Lihan, Ismail Bin Ahmad ,The Effect Of Combination Of Octadecanoic Acid, Methyl Ester And Ribavirin Against Measles Virus , International Journal Of Scientific & Technology Research. 2(2013) 2277-8616.

4. Tulloch .A.P , Mass Spectra Of Pyrrolidides Of Oxy, Hydroxy And Trimethylsilyloxy Octadecanoic Acids , Springer Published.20(1985)652–663.

5. Isac Paulraj .E,S.Muthu , Spectroscopic Studies (Ftir, Ft-Raman And Uv), Potential Energy Surface Scan, Normal Coordinate Analysis And Nbo Analysis Of (2r,3r,4r,5s)-1-(2-Hydroxyethyl)-2-(Hydroxymethyl) Piperidine-3,4,5-Triol By Dft Methods

,Spectrochimica Acta Part A: Molecular And Biomolecular Spectroscopy. 108 (2013) 38-49.
6.Muhammad Alihashmi ,Afsarkhan ,Khurshidayub,Umarfarooq , Spectroscopic And Density Functional Theory Studies Of 5,7,3',5'-Tetrahydroxyflavanone From The Leaves Of Olea Ferruginea , Spectrochimica Acta Part A: Molecular And Biomolecular Spectroscopy. 128 (2014) 225-230.
7. Singh .R ,R.A.Yadav , Raman And Ir Studies And Dft Calculations Of The Vibrational Spectra Of 2,4-Dithiouracil And Its Cation And Anion , Spectrochimica Acta Part A: Molecular And Biomolecular Spectroscopy. 130(2014) 188-197.
8. Coates, J. Encyclopedia of Analytical Chemistry, Interpretation of Infrared Spectra: A Practical Approach. (2000) 10881-10882.
9. Altun .A,K.Golcuk ,M.Kumru , Structure And Vibrational Spectra Of P-Methylaniline: Hartree-Fock, MP2 And Density Functional Theory Studies , Journal Of Molecular Structure: Theochem. 637 (1–3) (2003) 155-169.
10.Sathyanarayana.D.N, Vibrational Spectroscopy Theory And Applications, International (P) Limited Publishers,New Delhi(2004)4415.
11. Kalsi.P.S, Spectroscopy Of Organic Compounds, Wiley Eastern Limited, New Delhi, (1993) 117–118.
12.B.R. Raajaram, N.R. Sheela, S. Muthu, Investigation on 1-Acetyl-4(4-Hydro Xyphenyl pipperazine an anti-fungal drug by spectroscopic, quantum chemical Computations and molecular docking studies, J. Mol. Struct. 1173 (2018) 583–595.
13. Robert L. Pecsok, Lozand Donald Shields, McWilliams, Modern methods of chemical analysis. 2 (1976).
14. A.R. Prabakaran, S. Mohan, Indian, Molecular structure and vibrational investigation of benzenesulfonic acid methyl ester using DFT (LSDA, B3LYP, B3PW91 and MPW1PW91) theory calculations, J.Phys. 63B (1989) 468–473.
15. Krishnakumar .V,K.Murugeswari ,N.Surumbarkuzhali , Molecular Structure, Intramolecular Hydrogen Bonding And Vibrational Spectral Investigation Of 2-Fluoro Benzamide – A Dft Approach , Spectrochimica Acta Part A: Molecular And Biomolecular Spectroscopy. 114(2013) 410-420.
16. Fathima Rizwana .B ,Johanan Christianprasana ,Christina Susanabraham ,S.Muthu , Spectroscopic Investigation, Hirshfeld Surface Analysis And Molecular Docking Studies On Anti-Viral Drug Entecavir , Journal Of Molecular Structure 1164(2018) 447-458.
17. Murray.J.S, K.Sen,Molecular Electrostatic Potentials,Theoretical and Computational Chemistry. 1(1996)105-538.
18. Rajesh .P ,S.Gunasekaran ,S.Seshadri ,T.Gnanasambandan , Dft Computational Analysis Of Piracetam , Spectrochimica Acta Part A: Molecular And Biomolecular Spectroscopy. 132(2014) 249-255.
19. Rajesh .P ,S.Gunasekaran ,S.Seshadri ,T.Gnanasambandan ,Experimental And Theoretical Study Of Ornidazole , Spectrochimica Acta Part A: Molecular And Biomolecular Spectroscopy. 153(2016) 496-504.
20. Zuhal Ozdemir, H Burak Kandilci, Bulent Gumusel, Unsal Calis, A Altan Bilgin , Synthesis And Studies On Antidepressant And Anticonvulsant Activities Of Some 3-(2-Furyl)-Pyrazoline Derivatives, Eur J Med Chem. 42(3) (2007) 373-379.
21. Suresh Kumar .G.S ,A.Antony Muthu Prabu ,S.Jegan Jenniefer ,N.Bhuvanesh ,P.Thomas Muthiah ,S.Kumaresan , Syntheses Of Phenoxyalkyl Esters Of 3,3'-Bis(Indolyl)Methanes And Studies On Their Molecular Properties From Single Crystal Xrd And Dft Techniques , Journal Of Molecular Structure. 1047 (2013) 109-120.